CRISPR-PIN: Modifying gene position in the nucleus via dCas9-mediated tethering

Jyun-Liang Lin[a],[1], Holly Ekas[a], Matthew Deaner[a], Hal S. Alper[a],[b],*

[a] McKetta Department of Chemical Engineering, The University of Texas at Austin, 200 E Dean Keeton St. Stop C0400, Austin, TX 78712, USA
[b] Institute for Cellular and Molecular Biology, The University of Texas at Austin, 2500 Speedway Avenue, Austin, TX 78712, USA

ABSTRACT

Spatial organization of DNA within the nucleus is important for controlling DNA replication and repair, genetic recombination, and gene expression. Here, we present CRISPR-PIN, a CRISPR/dCas9-based tool that allows control of gene Position in the Nucleus for the yeast *Saccharomyces cerevisiae*. This approach utilizes a cohesin-dockerin interaction between dCas9 and a perinuclear protein. In doing so, we demonstrate that a single gRNA can enable programmable interaction of nuclear DNA with the nuclear periphery. We demonstrate the utility of this approach for two applications: the controlled segregation of an acentric plasmid and the re-localization of five endogenous loci. In both cases, we obtain results on par with prior reports using traditional, more cumbersome genetic systems. Thus, CRISPR-PIN offers the opportunity for future studies of chromosome biology and gene localization.

1. Introduction

The eukaryotic nucleus introduces an additional level of organization and control of gene expression not seen in prokaryotic counterparts. This temporal and spatial organization, along with coordination of cis-regulatory elements and trans-acting factors, ensures accurate nuclear events including DNA replication and repair, homologous recombination, and gene expression [1,2]. Elucidating and manipulating the three-dimensional architecture of the nucleus can thus play a significant role in understanding overall function. In analogous protein counterparts, primary sequence can provide information on motifs and homology [3] and secondary structure provides information on local structural features (like helices and sheets), whereas tertiary and quaternary structure provide an elucidated picture of distal site interactions, enzyme active sites, and allostery [4–6]. A similar picture is evident with DNA sequence-structure space with respect to gene expression. While primary sequence can provide information on key transcription factor binding sites [7] and secondary structure can be used to understand nucleosome and chromatin interactions with promoters and terminators [8–10], tertiary structure in the genome can provide a much more lucid picture of gene expression [11,12]. For instance, the localization of galactose-inducible *GAL1* to the nuclear

pore complex (NPC) has been shown to be both necessary and sufficient to dampen its induction in galactose and ensure rapid repression when transferred to glucose [13]. It has also recently been demonstrated that disruption of genes responsible for anchoring telomeres to the nuclear envelope (*YKU70* and *ESC1*) causes misregulation of 60 genes, highlighting the utmost importance of nuclear localization in controlling gene expression for subtelomeric genes in particular [14]. Towards greater understanding, a few genetic tools have been used to study the impact of chromosome organization at the nuclear periphery, especially for the case of interrogating spatial effects on gene expression at the single gene [15–18] or chromosome level [19] and in enabling acentric plasmid segregation [20,21]. However, new synthetic tools that enable programmable spatial organization of chromosomes would help progress future studies into these phenomena.

The vast majority of work in the field relies on TetO-TetR, LacO-LacI, or LexA-LexA binding site based tethering of DNA [16,18,20,21]. However, these approaches are severely limited in scale and scope for a number of reasons. First, the initial construction and genomic integration of repetitive TetO or LacO arrays to tether loci using TetR or LacI (respectively) is time-consuming, remains difficult using standard cloning methods in recombinase-proficient bacteria, and causes genomic instability in the host organism [21]. Second, it is highly

---

laborious to localize multiple genetic loci to the same spot, as each genetic locus must be pre-modified to incorporate a TetO/LacO array. Third, sizable integrated arrays can introduce a rather large perturbation to DNA structure and function. Thus, new synthetic tools are required that can program genome localization without the need for large, repetitive sequence elements or other genome modifications.

To address these challenges, we present a new synthetic approach based on the widely used CRISPR/dCas9-system that can enable gene positioning in the nucleus (CRISPR-PIN). Specifically, we utilize the cohesin and dockerin interaction to link together a dCas9 protein fused to a cohesin domain with a nuclear membrane protein tagged with dockerin. In such a manner, expression of a guide RNA (gRNA) enables specific re-localization of a genomic locus to the nuclear periphery. This method enables facile and non-invasive control of chromosome organization as it solely requires expression of dCas9 coupled to a cohesin domain, a gRNA, and a nuclear protein fused with a dockerin domain. Each of these elements can be encoded within a simple plasmid. While similar to a recently published approach for CRISPR-mediated gene positioning [22], CRISPR-PIN offers 3 unique differences: 1) dCas9 and sgRNA are both expressed from a plasmid, allowing easy localization without the need for stable integration and expression, 2) CRISPR-PIN relies on a constitutive cohesin-dockerin interaction, mitigating the need for chemical inducers, and 3) CRISPR-PIN is the first technique to allow control over gene positioning in yeast, an important eukaryotic model. After demonstrating that all parts of the CRISPR-PIN system are functional, we investigate two case studies. First, we demonstrate the successful localization and segregation of an acentric plasmid (a plasmid lacking centromere). Second, we demonstrate the successful reorganization of chromosomal gene positions. In both cases, the results obtained here match those obtained using traditional TetR and LexA DNA binding methods reported in the literature. Thus, this work showcases the first usage of a CRISPR/dCas9 system for control of chromosome spatial organization and gene position in yeast.

2. Methods

2.1. Strains, media, and culture conditions

E. coli DH10β was used for all molecular cloning except for plasmids containing the LacO or TetO array, which were carried with MAX Efficiency® Stbl2™ (Invitrogen) and NEB® Stable Competent *E. coli* (New England BioLabs Inc.), respectively. LB medium containing $50 \, \mu g \, mL^{-1}$ of ampicillin was used to grow DH10β while SOC medium was used to grow Stbl2 and Stable Competent cells. DH10β cells were grown at 37 °C while Stbl2 and Stable Competent cells were grown at 30 °C.

S. cerevisiae strains used in this study are listed in Tables S1–2. All modified yeast strains were isogenic to BY4741. Yeast rich medium (YPD) and synthetic complete medium (SD) containing 0.67% yeast nitrogen base, complete supplement mixture (CSM) with appropriate dropout, and 2% glucose were used to culture yeast.

2.2. Plasmid and yeast strain construction

Plasmids used in this study are listed in Table S3. Cloning techniques including Gibson assembly and yeast recombination were used to assemble DNA fragments into the vectors. Promoters (HXT3, ENO1, and TEF1), genes (*HXK1*, *ABP1*, *IDI1*, *SAC7*, and *SCO2*) and terminators (ADH1 and PRM9) were amplified from yeast genomic DNA. dCas9 of *S. pyogenes* was amplified from pAL115 while SNR52 promoter and SUP4 terminator were amplified from pAL279. YFP, and cohesin and dockerin of *C. thermocellum* were amplified from pAL22. mCherry was amplified from pAL13. BFP gene was synthesized by IDT, and the sequence is provided in Table S4. TetO and LacO arrays were obtained from pAL15 and pAL37, respectively. TetR and LacI sequences were acquired from pAL32 and pAL124, respectively. gRNA sequences used for targeting of BFP were included in Table S5.

Yeast strains were established by methods including CRISPR/Cas9-mediated markerless integration, PCR-mediated epitope tagging with the selection marker, and integration of linearized yeast-integrating vectors. For integration of cargo fragments, 50 bp homologous sequences were used for genetic recombination. To construct YS235, *mCherry-CYC1t-MET15* amplified from pAL205 was tagged to 3′ end of *NUP49*. To construct YS229 and YS251, P_{HIS3}-GFP-LacI amplified from pAL124 and P_{LEU2}-TetR-YFP amplified from pAL32 were integrated to *TRP1* site of YS235 individually. To construct YS476, YS527, YS533, YS535, and YS537, linearized plasmids of pAL476, pAL527, pAL533, pAL535, and pAL537 were integrated to the genomic loci of *HXK1*, *ABP1*, *IDI1*, *SAC7*, and *SCO2*, respectively. To construct YS258, P_{TEF1}-BFP-T_{PRM9} amplified from pAL215 was inserted to *YPL062W* site, and the linearized pAL244 was integrated on the 3' of the expression cassette. All linearization of integrating plasmids was carried out on a unique restriction site in the genes. All genomic modifications were confirmed by colony PCR.

2.3. Confocal microscopy analysis

Yeast strains for confocal analysis were inoculated from glycerol stocks into 1 mL of SD -URA medium and grown for 24 h in a 96-well deep well plate at 30 °C. After 24 h, cells with an initial OD_{600} of 0.05 were transferred to 1 mL of fresh SD – URA in the same plate and grown for additional 20 h at 30 °C. To prepare samples for imaging, 300 μL of the cell culture was spun down, 270 μL of the supernatant was removed, and cells were resuspended with the residual medium. Finally 1 μL suspension was mounted on the slide for imaging.

Cells were imaged by Zeiss LSM 710 confocal microscopy equipped with a Plan-Apo 63X/1.4 Oil DIC M27 objective lens, and Zen software. GFP, YFP, and mCherry were excited with lasers at 488 nm, 514 nm, and 561 nm and emitted in the ranges of bandpass at 485–621 nm, 519–583 nm, and 582–754 nm, respectively. Z-stack acquisition was used to cover the entire nuclear volume, in which over 7 slices with an interval of 0.41 μm were harvested. Nuclear localization of genes was determined by images that displayed clear nuclear morphology and gene position.

2.4. Plasmid stability test

Cells were grown overnight in SD –U –H medium at 30 °C. Next day the cultures were diluted 1:50 to YPD medium and grown for 9 h at 30 °C. Cells were then washed with either SD –U –H or SD –U twice and roughly 500 cells were plated on the SD plates with the same nutrient dropout. Three independent plates were analyzed for each strain. Images of plates were taken after formation of appropriate colony sizes, and the number of colonies formed was quantified by ImageJ. Plasmid stability measures the percentage of cells containing the acentric plasmids after non-selective growth, which is defined as the number of colonies formed on selective SD –U –H plates divided by the number of colonies on non-selective SD –U plates.

2.5. Spot assay

The same strains used for the plasmid stability test were used for the spot assay. Cells were grown overnight in SD –URA –HIS at 30 °C. Next day, cell density was measured and 0.8 OD_{600} cells were resuspended in the same medium. The cell suspension was serially diluted by 10-fold, and four concentrations were prepared for the assay. Three microliter cells of each suspension were spotted on SD –URA –HIS plates and grown at 30 °C until reaching appropriate colony sizes. The image was taken by Molecular Imager® Gel Doc (BIO-RAD).

2.6. Statistical analysis

To measure statistical significance between no gRNA controls and

gRNA expressed, Welch's independent 2-sample *t*-test was run using SAS software (SAS Institute, Cary, NC). For all t-tests each sample was assumed to be normal and independently sampled. For Fig. 2, ANOVA was first run to confirm statistical difference between the strains and then four pairwise 2-sample t-tests were run with a Bonferroni correction.

3. Results and discussion

3.1. Re-localization of dCas9 to the nuclear periphery using a cohesin-dockerin interaction

Our first goal was to construct a system that would allow tethering of dCas9 to the nuclear periphery via protein-protein interactions. To establish this system, we chose the endonuclease-null version of *Streptococcus pyogenes* Cas9 (dCas9) [23] and confirmed that heterologous expression of dCas9 fused with a nuclear localization sequence (NLS) results in nucleoplasmic localization (Fig. S1). In this study, we opted to localize genes to the nuclear periphery through interactions with the nuclear membrane protein, Esc1p. To do so, we made use of a synthetic protein scaffold consisting of cohesin (Coh) and dockerin (Doc) from *Clostridium thermocellum*, an interaction previously used to localize enzymes to the surface of lipid droplets [24]. Here, we adapted this strategy by enabling an interaction between a dCas9 protein fused with Coh and the nuclear membrane protein Esc1p fused with Doc. We visualized the interaction and resulting nuclear localization of the proteins by also fusing a yellow fluorescent protein (YFP) to the middle of dCas9-Coh and mCherry at the C-terminus of Esc1-Doc (Fig. 1a). Confocal microscopy analysis of both Esc1-mCherry (control) and Esc1-Doc-mCherry showed ring-like structures, indicating proper localization at the nuclear periphery. When both dCas9-YFP-Coh and EscI-Doc-mCherry were co-expressed, microscopy uncovers overlapping fluorescent rings indicative of co-localization at the nuclear periphery. In contrast, in the absence of fused Doc, dCas9 was found to be nucleoplasmic (Fig. 1b). Finally, we found that the inheritance pattern of dCas9-YFP-Coh from mother to daughter cells followed the same pattern as Esc1-Doc-mCherry (Fig. S2), indicative of a strong association between dCas9 and Esc1. For simplicity, we use the term "CRISPR-PIN" in the remainder of this work to describe the involvement of dCas9-Coh and Esc1-Doc, even though we envision many other such interactions between dCas9 and other nuclear proteins at the periphery and pore.

3.2. Re-localization and segregation of an acentric plasmid using CRISPR-PIN

After establishing an approach to localize dCas9-Coh to the nuclear periphery, we next sought to demonstrate that the tripartite interaction between dCas9, gRNA, and DNA can be used to localize desired DNA and result in a concurrent phenotypic change. Previous work suggests that acentric plasmids can be specifically segregated to daughter cells via association with the nuclear envelope [25]. Here, we challenged our CRISPR-PIN approach to artificially tether an acentric plasmid to the nuclear envelope in an effort to enabled synthetic plasmid maintenance in the cell.

We utilized a traditional LacO/LacI array to visualize the localization of the acentric plasmid in the nucleus. Specifically, by cloning the LacO array onto the plasmid and co-expressing the LacI transcriptional repressor fused to GFP (GFP-LacI), we were able to track plasmid localization via confocal microscopy. Next, we defined the boundary of the nuclear envelope through expressing a nuclear pore complex protein (Nup49p) fused with mCherry (Nup49-mCherry). Finally, we defined perinuclear localization of the acentric plasmid as the case when the fluorescent signal from GFP-LacI overlapped with the Nup49-mCherry signal. Using the CRISPR-PIN approach, we expressed dCas9-Coh and Esc1-Doc as well as a gRNA targeting the acentric plasmid and obtained 62.6 ± 1.0% (standard deviation) perinuclear plasmid localization, while the no gRNA control only exhibited 44.5 ± 3.2% perinuclear localization (Fig. 1c and d). While the no gRNA control maintained a somewhat high level of perinuclear localization, we hypothesize that this is due to the large surface area of the nuclear periphery relative to the nucleoplasm and note that most constructs tested in our study were randomly localized at the nuclear periphery in roughly 30–50% of cells.

To test the phenotypic response of this localization, we conducted a
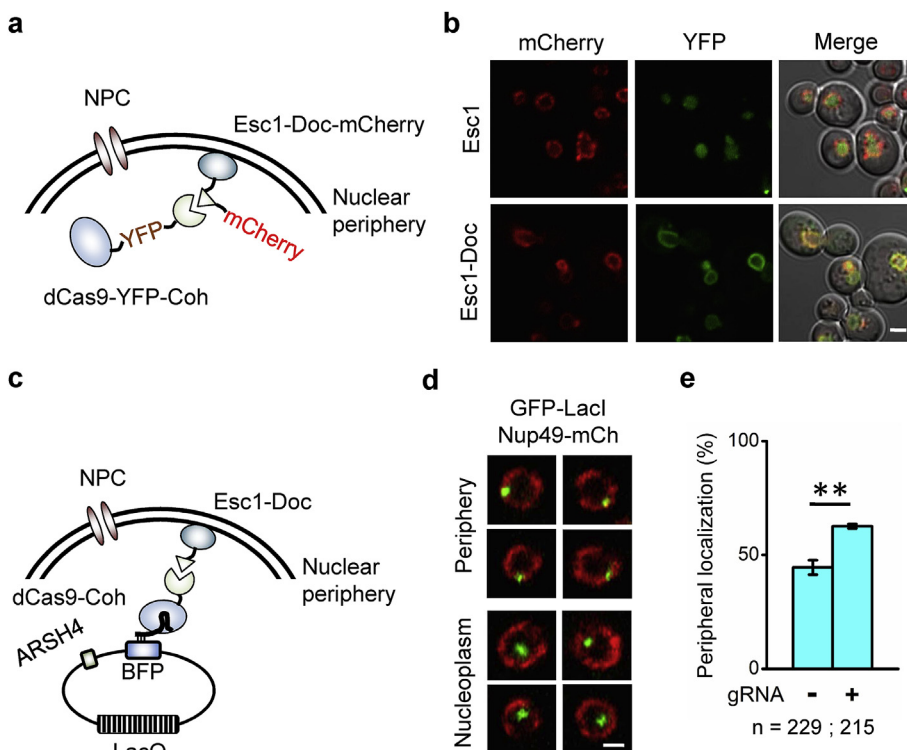
Fig. 1. Development of CRISPR-dCas9-based gene positioning in the nucleus (CRISPR-PIN). (a) A schematic diagram showing the strategy to localize dCas9 (*Streptococcus pyogenes*) to the yeast nuclear periphery. Abbreviations: NPC, nuclear pore complex; Coh, cohesin; Doc, dockerin; and YFP, yellow fluorescent protein. (b) Confocal microscopy analysis nuclear localization of dCas9-Coh. Esc1 is a perinuclear membrane protein. Scale bar: 2 μm. (c) A schematic diagram showing the design of perinuclear organization of the acentric plasmid. Abbreviations: ARSH4, autonomous replicating sequence; TEF1p, TEF1 promoter; BFP, blue fluorescent protein; PRM9t, PRM9 terminator; LacO: lac operator. (d) Confocal microscopy analysis and quantification of nuclear localization of the acentric plasmid. The acentric plasmid localization is visualized via expression of GFP-LacI, which binds to the LacO array. (e) Quantification of localization is compared based on image analysis similar to (d). Abbreviations: LacI, lac repressor; and mCh, mCherry. n represents number of counted cells from three independent samples (n = 3), and data are shown in mean and standard deviation. *P < 0.05, **P < 0.01, ***P < 0.001 by Welch's independent 2-sample *t*-test. Scale bar: 2 μm.
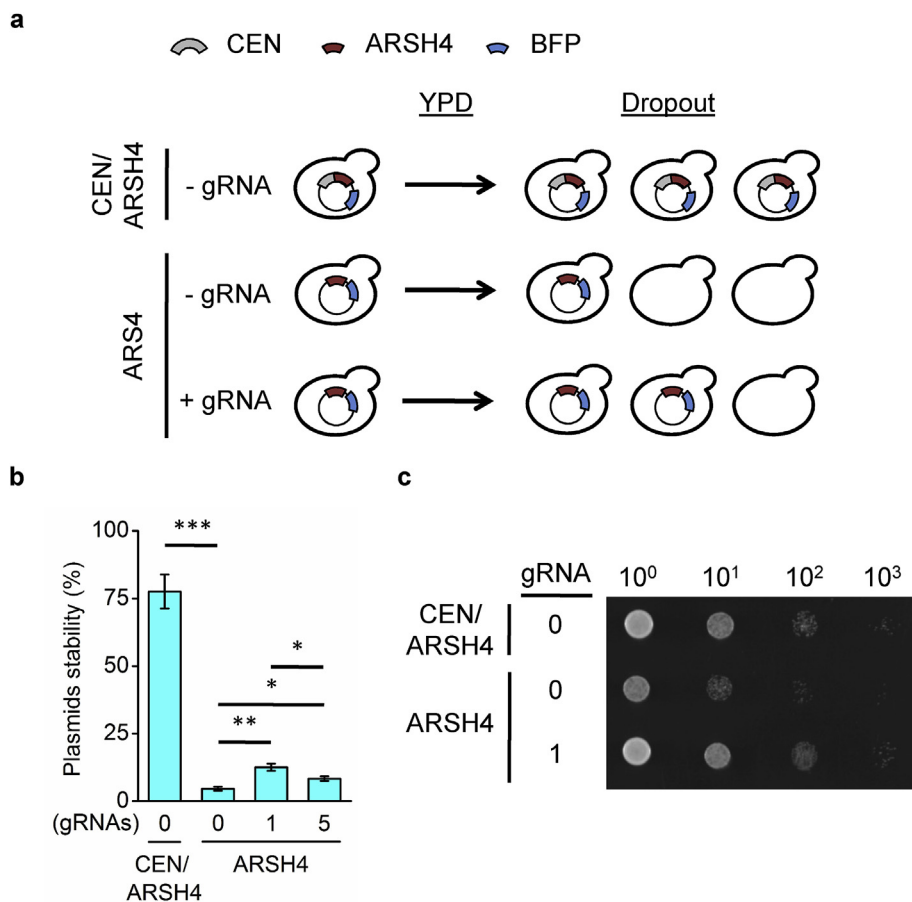
Fig. 2. CRISPR-PIN aids the segregation of acentric plasmid. (a) A schematic diagram depicting the concept of the plasmid stability test. Cells are co-transformed with the acentric plasmids and CRISPR-PIN. A control plasmid containing a centromere undergoes normal segregation, whereas the acentric plasmid lacking a centromere fails to segregate properly. The presence of CRISPR-PIN with expression of gRNA targeting the plasmid assists the mitotic process, resulting in more stable acentric plasmid segregation. Abbreviation: CEN, centromere; gRNA, single guide RNA. (b) Quantification of plasmid stability. Data are collected by counting three synthetic dropout plates (n = 3), and presented in mean and standard deviation. *P < 0.05, **P < 0.01, ***P < 0.001 by ANOVA followed by pairwise Welch's independent 2-sample t-tests with Bonferroni correction. (c) Spot assay of cells co-transformed the acentric plasmids and CRISPR-PIN. 10-fold serial dilutions of overnight-grown cells are spotted on synthetic dropout plates. Growth was restored using the CRISPR-PIN approach to a level on par with the centromeric plasmid.

series of plasmid segregation tests. These tests were conducted alongside a positive control plasmid containing a full CEN sequence. Auxotrophic markers of HIS3 and URA3 were used to select cells harboring the acentric (and control) and CRISPR-PIN plasmids, respectively. Overnight cultures were transferred into rich medium to test for plasmid stability and loss. After a period of 9 h, we evaluated the efficacy of CRISPR-PIN to segregate the acentric plasmid and provide mitotic stability of the plasmid on selection plates (Fig. 2a). In this test, cells harboring the plasmid with a functional centromere and the CRISPR-PIN plasmid showed 77.5 ± 6.3% plasmid stability. As expected, when the CEN sequence was removed, plasmid stability dropped to 4.6 ± 0.8%. Using the CRISPR-PIN system, we found that plasmid segregation increased to 12.6 ± 1.3%. This result and level of increase is commensurate with a previous study that fused the kinetochore component Dam1 to the transcriptional repressor TetR for binding to 10 copies of TetO sites on the acentric plasmid [20]. However, our approach was obtained with only a single gRNA site. Surprisingly, expression of multiple, distinct gRNAs targeted to the plasmid did not improve plasmid stability, suggesting a potential limitation of Esc1-Doc availability at the nuclear periphery or titration of effective gRNA (Fig. 2b).

Finally, we sought to test whether this level of plasmid segregation could enable sustained growth on selective medium. To do so, we measured the phenotypic effect of localization by a spot plate assay using –URA –HIS plates. In this assay, the CRISPR-PIN plasmid enabled maintenance of the acentric plasmid and nearly completely rescued the growth defect seen in a cell lacking gRNA expression (Fig. 2c). Thus, CRISPR-PIN enabled the proper segregation of an acentric plasmid and enabled a growth rate akin to the CEN-containing control. Overall, synthetic segregation of an acentric plasmid validated that CRISPR-PIN could affect a significant phenotypic change through localization to the nuclear periphery.

3.3. Re-localization of chromosomal loci using CRISPR-PIN

Having demonstrated artificial localization and segregation of plasmids, we next sought to localize endogenous chromosomal loci to the nuclear periphery. In this regard, we were motivated by prior studies whereby ectopic insertion of a single gene recruitment sequence (GRS I) has been shown to increase perinuclear localization of the *URA4* locus [26]. To utilize a singular gRNA design, we integrated the BFP gene downstream of each of our target loci. We used a similar approach to visualize gene position, in which TetR was fused with YFP, a TetO array was integrated downstream of BFP at each gene locus, and YFP localization was determined via confocal microscopy and used as a read-out of gene position (Fig. 3a). The effectiveness of our system was validated here by organizing a series of gene loci including *SCO2, ABP1, SAC7, HXK1,* and *IDI1*, which are located on chromosomes II, III, IV, VI, and XVI, respectively. As a point of comparison, a previous study incorporated the bacterial LexA protein fused with the C-terminal domain of Esc1 (LexA-Esc1^C) along with insertion of four LexA sites upstream of *HXK1*. In this construct, the perinuclear association was increased from near 60% to slightly over 80% when cultured in glucose-containing medium. Using our CRISPR-PIN approach, we observed a similar net increase of perinuclear localization from 51.3 ± 4.5% to 71.5 ± 4.2% with only a single gRNA site for localization. We also observed a similar net increase of 17%, 16%, 18%, and 15% perinuclear gene localization for *SCO2, ABP1, SAC7,* and *IDI1*, respectively (Fig. 3b–c). Thus, we believe that CRISPR-PIN can provide generalizable localization of desired genes simply by expressing a complementary gRNA.

3.4. Conclusion

Through this work we demonstrate a new synthetic biology tool termed CRISPR-PIN that can reorganize the chromosome and localize

a

b

TetR-YFP
Nup49-mCh

c
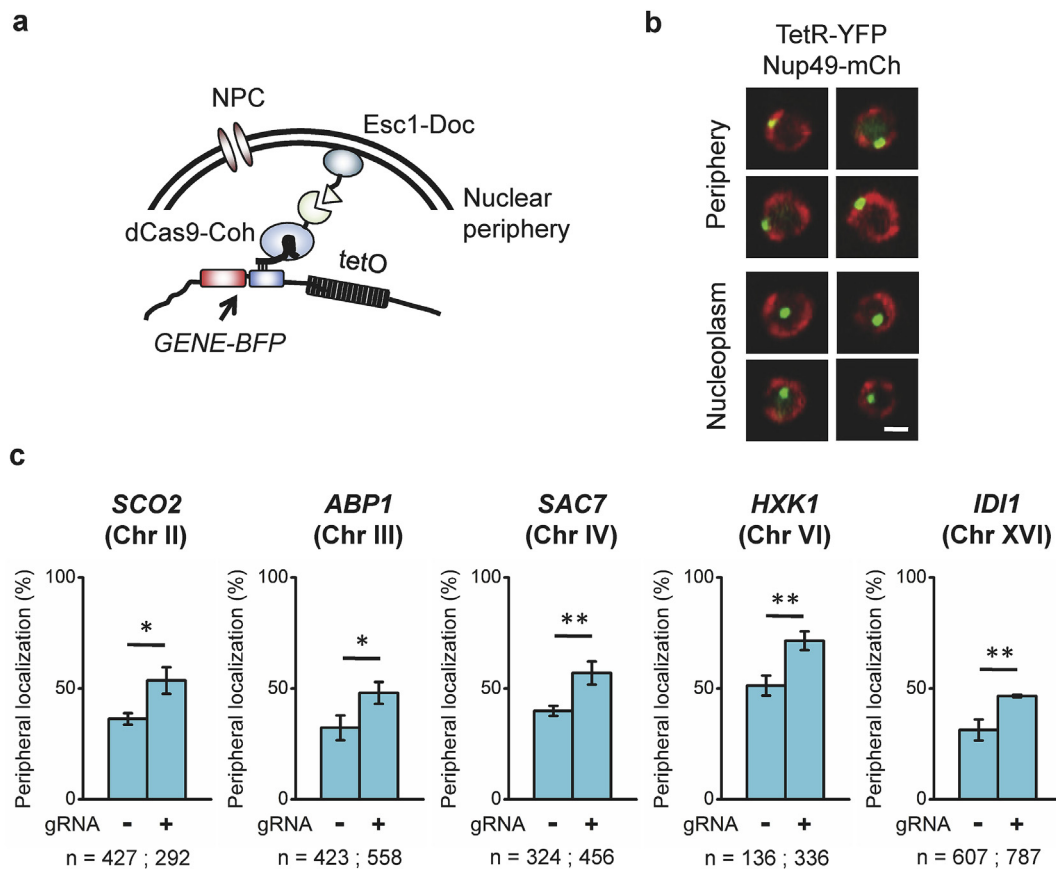
Fig. 3. CRISPR-PIN relocates the gene positions from various chromosomes. (a) The CRISPR-PIN approach is used to enable perinuclear localization of the target loci to the nuclear periphery. An array of TetO sites were integrated into the target loci for gene visualization. Abbreviation: TetO, Tet operator. (b) Representative fluorescence images showing perinuclear and nucleoplasmic localization of genes. Scale bar: 2 μm. (c) Quantification of nuclear localization of a series of genes. Chromosome number (Chr) of the gene is shown in Roman numerals. N represents number of counted cells from three independent samples (n = 3), and data are shown in mean and standard deviation. *$P < 0.05$, **$P < 0.01$, ***$P < 0.001$ by Welch's independent 2-sample t-tests between no gRNA controls and expressed gRNA targeted to each gene.

desired genes to the nuclear periphery in yeast. We demonstrate the phenotypic potential enabled by nuclear localization through segregation of an acentric plasmid. We further demonstrate the localization of 5 genes on different chromosomes to the nuclear periphery. In each of these cases, we obtain results commensurate with standard TetR or LexA DNA binding without their drawbacks. Thus, we believe our CRISPR-PIN strategy may be utilized as a powerful tool to study the effect of gene localization on desired phenotypes. Particularly, since our approach requires no genetic modification, it provides an facile method to alter the location of native chromosomal loci. It still remains to be investigated how gene loci tethered using CRISPR-PIN interact biophysically with the nuclear periphery to influence various phenotypes, but the current iteration of the technique has overcome the previous bottleneck of scalable and robust synthetic localization via the easy programmability of gRNAs. We thus foresee that CRISPR-PIN will enable new approaches in the fields of synthetic biology, chromosomal biology, and biomedical research.

Author contributions

JLL and HA conceived the study. JLL and MD designed and analyzed the experiments. JLL, MD, and HE conducted the experiments. All authors wrote the manuscript.

Notes

The authors declare no competing financial interest.

Appendix A. Supplementary data

Supplementary data to this article can be found online at https://doi.org/10.1016/j.synbio.2019.02.001.

References

[1] Misteli T. Beyond the sequence: cellular organization of genome function. Cell 2007;128:787–800.
[2] Baudat F, Imai Y, de Massy B. Meiotic recombination in mammals: localization and regulation. Nat Rev Genet 2013;14:794–806.
[3] de Juan D, Pazos F, Valencia A. Emerging methods in protein co-evolution. Nat Rev Genet 2013;14:249–61.
[4] Lee J, Natarajan M, Nashine VC, Socolich M, Vo T, Russ WP, Benkovic SJ, Ranganathan R. Surface sites for engineering allosteric control in proteins. Science 2008;322:438–42.
[5] Marsh JA, Teichmann SA. Structure, dynamics, assembly, and evolution of protein complexes. Annu Rev Biochem 2015;84:551–75.
[6] Laskowski RA, Gerick F, Thornton JM. The structural basis of allosteric regulation in proteins. FEBS Lett 2009;583:1692–8.
[7] Teixeira MC, Monteiro PT, Palma M, Costa C, Godinho CP, Pais P, Cavalheiro M, Antunes M, Lemos A, Pedreira T, Sa-Correia I. YEASTRACT: an upgraded database for the analysis of transcription regulatory networks in *Saccharomyces cerevisiae*. Nucleic Acids Res 2018;46:348–53.
[8] Morse NJ, Gopal MR, Wagner JM, Alper HS. Yeast terminator function can be modulated and designed on the basis of predictions of nucleosome occupancy. ACS Synth Biol 2017;6:2086–95.

[9] Curran KA, Crook NC, Karim AS, Gupta A, Wagman AM, Alper HS. Design of synthetic yeast promoters via tuning of nucleosome architecture. Nat Commun 2014;5:4002.

[10] Keung AJ, Joung JK, Khalil AS, Collins JJ. Chromatin regulation at the frontier of synthetic biology. Nat Rev Genet 2015;16:159–71.

[11] Lanctot C, Cheutin T, Cremer M, Cavalli G, Cremer T. Dynamic genome architecture in the nuclear space: regulation of gene expression in three dimensions. Nat Rev Genet 2007;8:104–15.

[12] Nguyen HQ, Bosco G. Gene positioning effects on expression in eukaryotes. Annu Rev Genet 2015;49:627–46.

[13] Green EM, Jiang Y, Joyner R, Weis K. A negative feedback loop at the nuclear periphery regulates GAL gene expression. Mol Biol Cell 2012;23:1367–75.

[14] Tokuda N, Sasai M. Heterogeneous spatial distribution of transcriptional activity in budding yeast nuclei. Biophys J 2017;112:491–504.

[15] Andrulis ED, Neiman AM, Zappulla DC, Sternglanz R. Perinuclear localization of chromatin facilitates transcriptional silencing. Nature 1998;394:592–5.

[16] Reddy KL, Zullo JM, Bertolino E, Singh H. Transcriptional repression mediated by repositioning of genes to the nuclear lamina. Nature 2008;452:243–7.

[17] Kumaran RI, Spector DL. A genetic locus targeted to the nuclear periphery in living cells maintains its transcriptional competence. J Cell Biol 2008;180:51–65.

[18] Taddei A, Van Houwe G, Hediger F, Kalck V, Cubizolles F, Schober H, Gasser SM. Nuclear pore association confers optimal expression levels for an inducible yeast gene. Nature 2006;441:774–8.

[19] Finlan LE, Sproul D, Thomson I, Boyle S, Kerr E, Perry P, Ylstra B, Chubb JR, Bickmore WA. Recruitment to the nuclear periphery can alter expression of genes in human cells. PLoS Genet 2008;4:e1000039.

[20] Kiermaier E, Woehrer S, Peng Y, Mechtler K, Westermann S. A Dam1-based artificial kinetochore is sufficient to promote chromosome segregation in budding yeast. Nat Cell Biol 2009;11:1109–15.

[21] Lacefield S, Lau DT, Murray AW. Recruiting a microtubule-binding complex to DNA directs chromosome segregation in budding yeast. Nat Cell Biol 2009;11:1116–20.

[22] Wang H, Xu X, Nguyen CM, Liu Y, Gao Y, Lin X, Daley T, Kipniss NH, La Russa M, Qi LS. CRISPR-mediated programmable 3D genome positioning and nuclear organization. Cell 2018;175. 1405-1417 e1414.

[23] Chavez A, Scheiman J, Vora S, Pruitt BW, Tuttle M, P R Iyer E, Lin S, Kiani S, Guzman CD, Wiegand DJ, Ter-Ovanesyan D, Braff JL, Davidsohn N, Housden BE, Perrimon N, Weiss R, Aach J, Collins JJ, Church GM. Highly efficient Cas9-mediated transcriptional programming. Nat Methods 2015;12:326–8.

[24] Lin JL, Zhu J, Wheeldon I. Synthetic protein scaffolds for biosynthetic pathway colocalization on lipid droplet membranes. ACS Synth Biol 2017;6:1534–44.

[25] Gehlen LR, Nagai S, Shimada K, Meister P, Taddei A, Gasser SM. Nuclear geometry and rapid mitosis ensure asymmetric episome segregation in yeast. Curr Biol 2011;21:25–33.

[26] Ahmed S, Brickner DG, Light WH, Cajigas I, McDonough M, Froyshteter AB, Volpe T, Brickner JH. DNA zip codes control an ancient mechanism for gene targeting to the nuclear periphery. Nat Cell Biol 2010;12:111–8.